THE ASTROPHYSICAL JOURNAL, 271:113–122, 1983 August 1

THE CHEMICAL INHOMOGENEITY OF THE SCULPTOR DWARF SPHEROIDAL GALAXY

GRAEME H. SMITH AND MICHAEL A. DOPITA
Mount Stromlo and Siding Spring Observatories, Research School of Physical Sciences, Australian National University
Received 1982 September 7; accepted 1983 January 20

ABSTRACT

Panoramic photometry of red giants in the Sculptor dwarf spheroidal galaxy is reported. By employing a narrow-band filter system designed to measure the absorption at the λ3883 CN band, and the Ca II H and K lines, Sculptor is found to be inhomogeneous with respect to both cyanogen and calcium. Furthermore, the Ca and CN enhancements are correlated, suggesting similarities between the enrichment process in Sculptor and the globular clusters ω Cen and M22.

Subject headings: galaxies: individual — galaxies: stellar content — stars: abundances

I. INTRODUCTION

Much of the recent interest in the dwarf spheroidal galaxies has been concerned with their chemical inhomogeneity. The color-magnitude diagrams of Draco (Stetson 1979; Zinn 1980*b*), Ursa Minor (Schommer, Olszewski, and Kunkel 1977; Zinn 1981; Schommer, Olszewski, and Cudworth 1981), Fornax (Demers, Kunkel, and Hardy 1979), and Sculptor (Norris and Bessell 1978) all appear to display giant branches wider than can be explained by the observational uncertainties alone. This suggests the presence of internal variations in the low-ionization-potential elements such as Fe, Si, and Mg (Renzini 1977). The existence of such variations in Draco was demonstrated by Zinn (1978), who found, from scanner observations of the line blanketed spectral region blueward of 5000 Å, an [Fe/H] abundance spread of $\sim$0.3 dex. This result was verified from measurements of Ca II H and K line strengths by Kinman, Kraft, and Suntzeff (1980), who in addition found giants apparently more metal-poor than those in M92. Variations in [Fe/H] were identified among four giants in Ursa Minor by Zinn (1981), on the basis of multichannel scanner observations, while spectra obtained of giants in Sculptor by Norris and Bessell (1978) show that [Fe/H] and/or [Ca/H] variations also exist within this system. The observations of van den Bergh (1969), Danziger (1973), Harris and Canterna (1977), and Zinn and Persson (1981), all indicate that a range of metal abundance exists among the globular clusters in Fornax.

The [Fe/H] and [Ca/H] inhomogeneities displayed by the dwarf spheroidals are reminiscent of those in the globular clusters ω Cen (Freeman and Rodgers 1975; Butler, Dickens, and Epps 1978; Rodgers *et al.* 1979; Norris 1980; Mallia and Pagel 1981; Cohen 1981; Gratton 1982) and M22 (Hesser and Harris 1979; Pilachowski *et al.* 1982; Norris and Freeman 1983). However, among the globular clusters these two appear to be unique in this way. Within most clusters variations in the spectroscopic appearance of carbon and nitrogen features—e.g., the $\lambda\lambda$3883 and 4215 CN bands and the λ4300 G-band—are common among red giants of similar temperatures and gravities, as outlined in the reviews by Kraft (1979), McClure (1979), and Freeman and Norris (1981), but these are not generally accompanied by large variations in the Ca or Fe abundance. The data available on C and N variations within dwarf spheroidals are very limited. Kinman *et al.* (1981) find from a sample of nine Draco giants that although this galaxy has the same mean [Fe/H] abundance as M92, its [C/Fe] is on the average three times that of M92, with one star having five times the mean M92 ratio. DDO photometry of five Draco giants by Hartwick and McClure (1974) shows none of the extreme CN band strengths characteristic of some ω Cen giants (see, e.g., Bessell and Norris 1976). A giant with strong G or CN bands was identified in Ursa Minor by Canterna and Schommer (1978), the nature of this star being further defined by Norris and Bessell (1978) and Zinn (1981). Norris and Bessell (1978), from spectra of one giant on the blue side and one on the red side of the Sculptor giant branch, found that the redder star had stronger λ3883 CN band and Ca II H and K line absorption, a property characteristic of ω Cen (Bessell and Norris 1976; Norris 1980) and M22 (Norris and Freeman 1982).

In view of the lack of any extensive survey of cyanogen band strengths among the dwarf spheroidals, such a program has been undertaken for the Sculptor galaxy, with a view to providing a cyanogen distribution for comparison with those now available for a number of globular clusters such as ω Cen (Norris 1980), NGC 6752 (Norris *et al.* 1981) and M22 (Norris and Freeman 1983). Considering also the [Fe/H] and [Ca/H] differences detected by Norris and Bessell (1978), a survey has also been made of the Ca II H and K line strengths. The combined CN and Ca data will provide a test for the hypothesis of Norris and Bessell that the Sculptor giants possess correlated Ca and CN inhomogeneities in a manner similar to those in ω Cen. The present observations consist of panoramic photometry employing a narrow-band filter system designed to measure the strength of the λ3883 CN band

and the Ca II H and K lines (see § II). The data reduction procedure is described in § III, while the results are presented in § IV and discussed in § V.

II. OBSERVATIONS

Observations were obtained in 1980 September and November by using the 3.9 m Anglo-Australian Telescope at f/8, with the Image Photon Counting System (IPCS; Boksenberg 1972) in the direct imaging mode. The photocathode of this device has a blue-enhanced S-20 response. Each image obtained was 440 × 440 picture elements (pixels) in format, with the scale of each frame being 0.″4–0.″5 pixel^{-1} E–W and 0.″5 pixel^{-1} N–S. Two fields in Sculptor were observed, with centers at (R.A., decl.)$_{1950}$ = (00:58:13, −33:59:57) and (00:58:05, −33:58:42). These will be designated fields 1 and 2, respectively, and were chosen to include in total about 80 of the stars from the color-magnitude diagram of Kunkel and Demers (1977).

Exposures were obtained through each of four narrow-band interference filters. Two of these have bandpasses of 36 Å and 31 Å FWHM with peak wavelengths (λ_c) of 3868 Å and 3905 Å, and are centered respectively on the λ3883 cyanogen absorption system, and a pseudo-continuum region between the CN system and the Ca II H and K lines. The filters are used to form a color equivalent to the spectroscopic $S(3839)$ cyanogen index of Norris *et al.* (1981). Observations of the cyanogen distribution among the subgiants in NGC 362, obtained using this filter system, are described by Smith (1983). Of the two other filters, one has λ_c = 3955 Å (FWHM = 43 Å) and the other λ_c = 4018 Å (FWHM = 33 Å). These are used respectively to measure the absorption in the Ca II H and K lines, plus a redward pseudo-continuum region.

On each run, observations of the dawn or dusk sky were obtained for the purpose of flat-fielding. These frames were smoothed with a 6 × 6 pixel half-width two-dimensional Gaussian filter, and normalized with the average counts per pixel, before dividing into the Sculptor images. This procedure corrects for coarse variations in the image tube response across the field, as well as for possible transmission variations across the interference filters. No attempt was made to correct for small-scale pixel-to-pixel variations in the image-tube response. All observations of Sculptor were made during dark of moon.

A typical example of the data is shown in Figure 1, which is a section from an exposure of field 2 through the λ3905 filter. Two exposures were obtained through the λ3868 and λ3905 filters for each of fields 1 and 2 during both the September and November observing runs. The exposures were typically of 1000 s duration, although 1500 or 2000 s exposures were occasionally made with the λ3868 filter. Observations of both fields were made with the λ3955 and λ4018 filters only in September.

III. DATA REDUCTION

Instrumental magnitudes were derived for the program stars by using the APEX panoramic photometry computer program written by Dr. E. B. Newell. A full description of the algorithms used in this program is presented by Newell (1979).

The data reduction, which is highly automated and run on the Mount Stromlo VAX 11/780 computer, takes place in several steps.

1. From the main 440 × 440 pixel^2 frames, smaller 31 × 31 pixel^2 arrays are extracted around each program star. It is on these subarrays that reduction proceeds.

2. The profiles of a sample of stars with well defined images are fitted by an analytic expression of the form

$$\psi(x) = a[(1 - Q)\exp(-\ln 2\beta) + Q/(\beta + 1)],$$

where $\beta = [2x/\Gamma]^2$, a is the height of the profile, and Γ is the full width of the profile at half height. This is a Lorentzian-Gaussian profile, with the size of the Lorentzian wings determined by the parameter Q. Average values of Γ and Q were computed for each 440 × 440 frame. Typical values of Γ, which is the parameter that reflects the seeing, and controls all size-dependent aspects of the APEX software, were from 2.5 to 4 pixels.

3. The centers of the program stars within their individual 31 × 31 pixel^2 arrays are next determined. First the sky intensity is determined from an annular zone around each star. Sky-subtracted intensity distributions are then determined along two mutually perpendicular strips centered on the approximate position of the star. The precise center of the star is determined from the peaks in the cross-correlation function obtained by cross-correlating these distributions with the standard profile $\psi(x)/a$. The centering routines were found to be successful for $\gtrsim 80\%$ of the program stars in each frame. The centers determined in this way could be visually inspected on a RAMTEK gray-scale display monitor linked to the VAX, and manually altered if deemed necessary. In cases where the centering algorithms were unsuccessful, the centers were judged by eye.

4. Stellar magnitudes are calculated by summing up intensities within concentric circles. A sequence of 10 such circles with radii incremented by $\Gamma/4$ is laid down, centered on the star, while an annulus of larger radius is used as a sky zone. A distribution of intensities is derived from all pixels whose centers lie within the sky zone, and the mode of this distribution I_s is used as the sky intensity. Newell (1979) has shown that this mode reliably takes account of stellar contamination in the sky zone providing that crowding is not too severe (see also Smith 1983). Such crowding is not a problem with the present data, since in general the extracted 31 × 31 pixel^2 arrays contained either no star or only one other star in addition to the program star. The magnitude of the star within the nth circle, m_n (where n = 1 to 10) was calculated from the relation

$$m_n(\lambda_c) = 25.0 - 2.5\log_{10}\left[\sum_{k=1}^{m} I_k - mI_s\right],$$

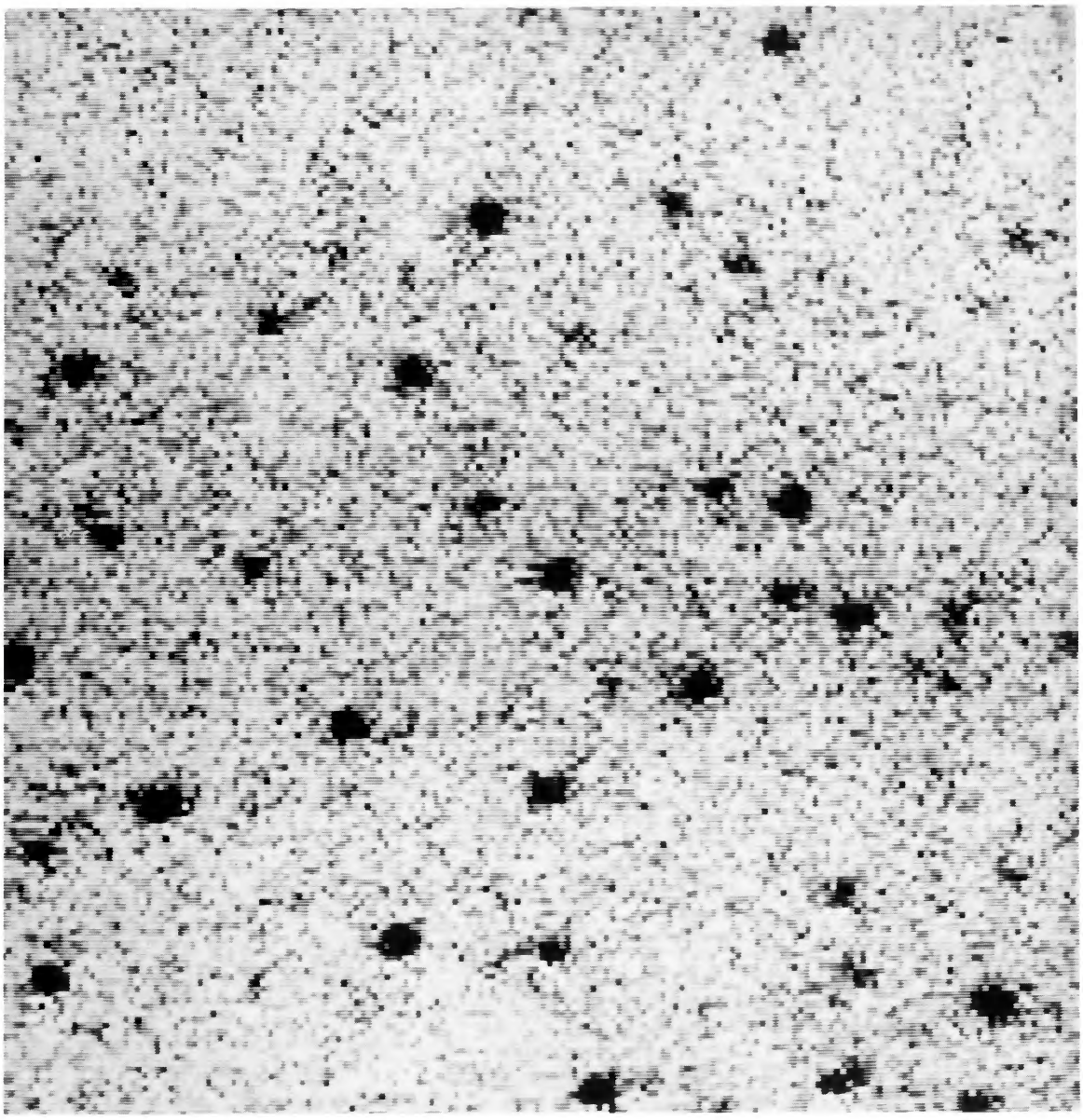

FIG. 1.—A 180 × 180 pixel^2 gray-scale display of a region in field 2, obtained through the 3905 Å filter

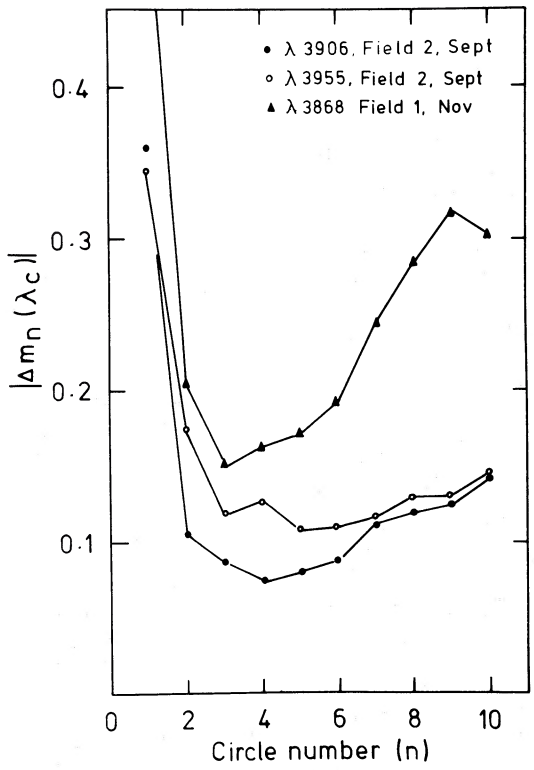

FIG. 2.—A plot of the mean absolute value of the magnitude differences (after correcting for a systematic difference) between two exposures of the same field plotted versus ring number. Each curve is designated by the filter through which the two exposures were made, the field observed, and the month in which the observations were made. The purpose of the plot is to show that the repeatability between exposures is optimized for magnitudes measured within aperture four.

where m is the total number of pixels included within the nth circle, and I_k is the intensity recorded in the kth pixel.

Ten magnitudes are therefore calculated for each star, requiring a decision as to which one of these to use. This was made by inspecting the repeatability of the individual stellar magnitudes obtained from two exposures of the same field, as a function of aperture size. An example of such data is shown in Figure 2, where the mean absolute value of the magnitude differences between two exposures, $|\Delta m_n(\lambda_c)|$, averaged over all stars in the field, and allowing for systematic differences, is plotted versus circle number. Each curve is defined by the filter through which the two exposures were made, the field observed, and the month in which the observations were made. These curves were found to reach a minimum near circle 4 (radius = Γ), which was therefore chosen as the aperture from which all magnitudes were taken. Since the size of this circle scales with the stellar profile half-widths, which are determined for each exposure, all measurements sample the same region of the stellar images.

IV. RESULTS

a) The Cyanogen Indices

Once magnitudes were obtained from each 440 × 440 pixel^2 frame, they were combined in the following way. The magnitudes measured from the two exposures per filter of each field were added together, and a cyanogen index

$$s_{CN} = m(3868) - m(3905)$$

was calculated, giving four sets of such colors, i.e., for the two fields observed in both November and September. The colors from these two months were then averaged, producing a set of s_{CN} values for fields 1 and 2. A sample of 14 stars exist in common between the two fields, which were chosen to provide some overlap, from which the mean difference Δs_{CN}(field 1 minus field 2) was calculated. This was treated as the systematic difference between the color systems defined by the two fields, and used to transform the field 2 values onto the field 1 system. The uncertainty in this difference is 0.03 mag.

The results are given in Table 1. Column (1) gives the Kunkel and Demers (1977) star number, columns (2) and (3) give the V and $B-V$ photometry obtained from Kunkel and Demers, column (4) gives the s_{CN} color (on the field 1 system) for each star, while column (6) indicates whether the star is placed in field 1, field 2, or both. Where a star was situated in both fields, its field 1 and transformed field 2 colors were averaged.

The uncertainty in the data can be assessed in a number of ways. Figure 3 shows a plot of September minus November s_{CN} colors as a function of V magnitude for both fields, corrections having first been made for systematic differences between the two months. Brighter than $V = 19.5$ the photometry generally repeats to better than 0.2 mag, but fainter than this limit much larger errors are incurred. Averaging the quantity $r = |s_{CN}(\text{Sept}) - s_{CN}(\text{Nov})|$ over all stars in each field, gives $r_m = 0.18$ for field 1, and $r_m = 0.16$ for field 2. Since the final s_{CN} values are averages over the November and September runs, the theory of small sample statistics (Keeping 1962) indicates that the standard error in these mean colors ($\sim 0.63 r_m$) is 0.12 for field 1, and 0.10 for field 2. An independent estimate of the errors can be obtained by assuming that the red horizontal-branch stars have the same s_{CN} values. This assumption is supported by the work of Smith (1983), who finds no evidence for an intrinsic variation in s_{CN} among the red horizontal branch (RHB) stars in NGC 362, for which $B-V < 0.7$, these stars being too hot to show significant CN bands. The observational error is then estimated to be the standard deviation in the distribution of the RHB star s_{CN} colors given in Table 1, which is 0.10. Finally, if the difference in the field 1 and field 2 s_{CN} values for the 14 stars in common is considered, a standard deviation of 0.06 is calculated to be appropriate for those stars with only a field 1 or a field 2 color, while a standard error in the mean of 0.04 is more appropriate to those stars found in both fields, these estimates being an average over the 14 stars.

TABLE 1

DATA FOR 72 SCULPTOR GIANTS

Star	V	B-V	S_{cn}	S_{ca}	Field	Star	V	B-V	S_{cn}	S_{ca}	Field
107[a]	20.27	0.32	0.24	-0.12	1	184	19.35	0.70	0.26	-0.05	1,2
108	20.22	0.71	0.37	0.12	1	185	20.11	0.62	0.17	0.21	1,2
111	19.31	0.82	---	0.16	1	186	20.11	0.72	0.26	0.04	1,2
112	19.90	0.80	---	0.19	1	187[a]	20.02	0.50	0.44	-0.05	1,2
119	18.14	1.10	0.43	0.32	1	188	20.10	0.63	0.32	-0.06	1,2
120	19.45	0.95	0.57	0.51	1	189	19.10	0.90	0.36	0.30	1,2
121	19.82	0.86	0.44	-0.06	1	190	19.27	0.97	0.33	0.53	1
123	17.73	1.13	0.40	0.42	1	191	18.35	1.05	0.32	0.26	1
126	17.35	1.32	0.46	0.59	1	192	19.30	0.89	0.24	0.16	1
128[a]	20.40	0.24	0.30	0.10	1	194	19.16	0.59	0.43	0.33	1
129	20.13	0.71	0.13	0.31	1	209	19.96	0.83	-0.01	-0.17	2
130	19.77	0.76	0.27	0.04	1	210[a]	19.93	0.51	0.14	-0.03	2
142	19.89	0.85	0.54	0.08	1	212	19.31	1.03	0.11	0.17	2
143	20.02	0.77	0.09	-0.10	1	231	19.79	0.67	0.06	-0.17	2
146	19.26	0.93	0.24	0.34	1	233	18.99	0.93	0.20	0.15	2
147	20.51	0.62	0.21	0.05	1	305	18.63	1.19	0.58	0.52	1
148	19.88	0.88	-0.20	0.18	1	306	20.24	0.63	0.18	---	1
149	18.64	0.95	0.37	0.11	1	312	19.37	0.87	0.67	---	1
152	19.36	0.68	0.32	0.08	1	313	19.63	0.83	0.26	0.33	1
153[a]	20.12	0.35	0.27	0.10	1	314	18.27	1.04	0.77	0.33	1
154	18.93	0.83	0.33	0.24	1	315	19.36	0.98	0.39	0.41	1
156[a]	20.17	0.34	0.30	0.12	1,2	316	19.73	0.85	0.12	0.33	1
158	19.78	0.72	0.30	0.11	1	317[a]	20.17	0.46	0.42	-0.14	1
160	18.66	0.95	0.38	0.33	1	318	19.66	0.96	0.21	0.48	1
161	17.75	1.14	0.36	0.35	1	327	18.24	1.19	0.35	---	1
162	19.86	0.85	0.46	0.25	1	328	17.20	1.40	0.48	0.50	1,2
169	19.84	0.59	0.48	0.05	1	329	17.64	1.08	0.53	0.66	1,2
171	20.01	0.79	0.59	0.17	1	330	17.36	1.50	0.56	0.65	2
174	19.36	0.88	0.21	0.23	1	331	18.05	1.04	0.44	0.19	2
177	19.00	0.98	0.23	0.39	1	332	17.52	1.37	0.43	---	1,2
178	19.93	0.91	0.12	0.38	1	333	17.51	1.24	0.48	0.33	2
179	20.14	0.71	0.47	0.30	1	334	18.62	0.95	0.22	0.24	2
180	18.98	0.87	0.45	0.32	1	335	18.07	1.20	0.49	0.46	2
181	19.93	0.65	0.23	0.04	1,2	336	17.21	1.41	0.41	0.51	2
182	19.84	0.95	0.50	0.48	1,2	337	17.39	1.51	0.38	0.62	2
183	19.98	0.90	0.26	0.05	1,2	340	18.30	1.10	0.38	0.32	2

[a] Denotes horizontal branch star.

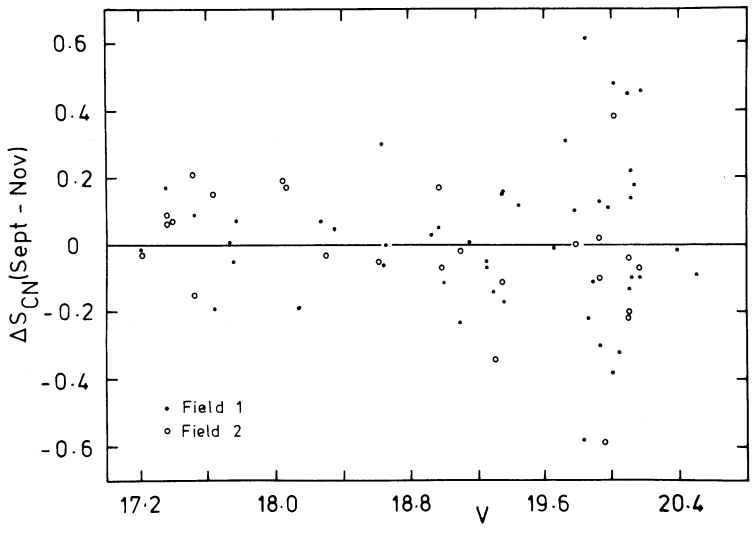

FIG. 3.—The differences between September and November s_{CN} colors for fields 1 and 2 are plotted as a function of V magnitude. This diagram illustrates the uncertainty in the cyanogen colors.

b) The Calcium Indices

A calcium color was formed as

$$s_{Ca} = m(3955) - m(4018) .$$

This is similar in concept to the spectroscopic m_{HK} index of Suntzeff (1980), although the bandpasses and central wavelengths are different. The values of s_{Ca} are given in column (5) of Table 1, where a constant has been added to the field 2 values to transform them onto the field 1 system. The error in this constant, which is derived from 13 common stars, is ± 0.05 (s.e.).

Figure 4 gives an idea of the uncertainty in the data. The absolute values of the differences between the two $m(3955)$, as well as the two $m(4018)$ magnitudes for field 1 are shown, where again the deterioration in the quality of the photometry at faint magnitudes is apparent. Since no data are available from November, the uncertainty in s_{Ca} is estimated from the difference in the field 1 and field 2 colors for those stars in common. This indicates an error of $\sim \pm 0.12$ for those stars located in only one field, and ± 0.08 for those in both. The standard deviation of the red horizontal branch star s_{Ca} values is 0.11.

V. DISCUSSION

The V, $B-V$ color-magnitude diagram of the Sculptor galaxy is plotted in Figure 5 from the data of Kunkel and Demers (1977). The stars represented in Table 1 are shown in Figure 5 as open circles. Also included on the diagram is a hand-drawn fit to the mean giant branch, which is defined for $V \geq 18.0$ by

$$(B-V)_m = -0.154V + 3.901 .$$

(Note that star 194 has been excluded from further analysis. Relative to the mean giant branch it is bluer by $\gtrsim 0.1$ mag in $B-V$ than any other non-horizontal branch star in Table 1. It is possibly a field star or an asymptotic giant branch (AGB) star. In view of the problem of defining the asymptotic branch in the Draco dwarf spheroidal (Stetson 1979, 1980; Zinn 1980*b*) and the possibility that very metal-poor stars may exist in the dwarf spheroidals, no other giants in Table 1 have been excluded from analysis as being either suspected field or AGB stars.)

A plot of s_{CN} versus V is shown in Figure 6. A baseline to the data, with the equation

$$s_{CN,0} = -0.142V + 2.833$$

is also shown. Relative to this line the cyanogen excess

$$\delta s_{CN} = s_{CN}(V) - s_{CN,0}(V)$$

is measured, in an identical manner to the $\delta S(3839)$ parameter of Norris *et al.* (1981) and Norris and Freeman (1983). A generalized histogram (see Searle and Zinn 1978) of δs_{CN} values is shown in Figure 7. The convolving Gaussian kernel has a dispersion of 0.05 (i.e., $\sim 0.5\ \sigma$), and so does not artificially broaden the distribution to any significant extent. Figures 6 and 7 indicate that Sculptor contains cyanogen-enhanced giants. Restricting attention to stars with $V < 19.6$ (in view of Fig. 3), it is apparent that stars 120, 305, 314, and 312 have strong cyanogen bands. The δs_{CN} values for these stars are 0.50, 0.39, 0.53, and 0.59, respectively, which represent an $\sim 3\ \sigma$ increase above the mean δs_{CN} defined by the remaining stars in this magnitude range (δs_{CN}[mean] $= 0.14 \pm 0.10$).

Norris and Smith (1981) have reviewed the cyanogen distributions for 10 globular clusters. It is apparent from comparing Figure 7 with their Figures 1 and 2 that Sculptor contains a smaller proportion of CN-enriched stars than most globular clusters, the exception being M55 (Smith and Norris 1982). This is the first

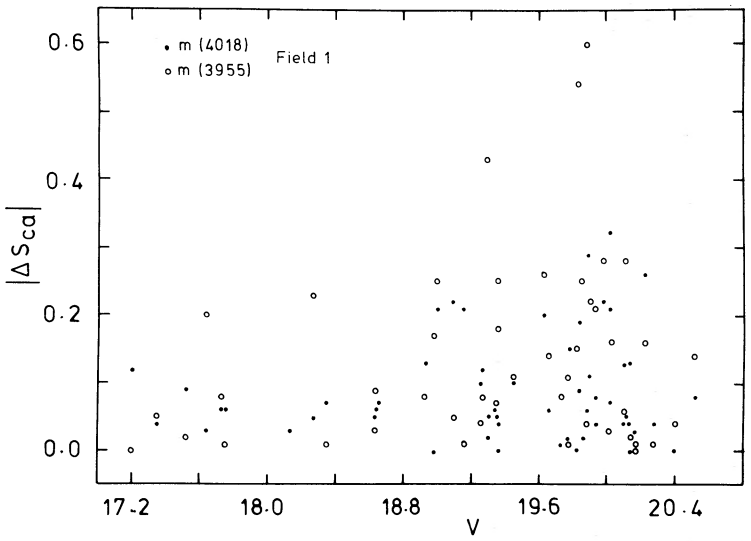

FIG. 4.—The uncertainty in the s_{Ca} calcium colors is indicated by this diagram, which shows the absolute values of the differences between the two measurements of the $m(3955)$ magnitudes, obtained from the September observations of field 1, plotted against V. Also shown are the differences between the two $m(4018)$ measurements.

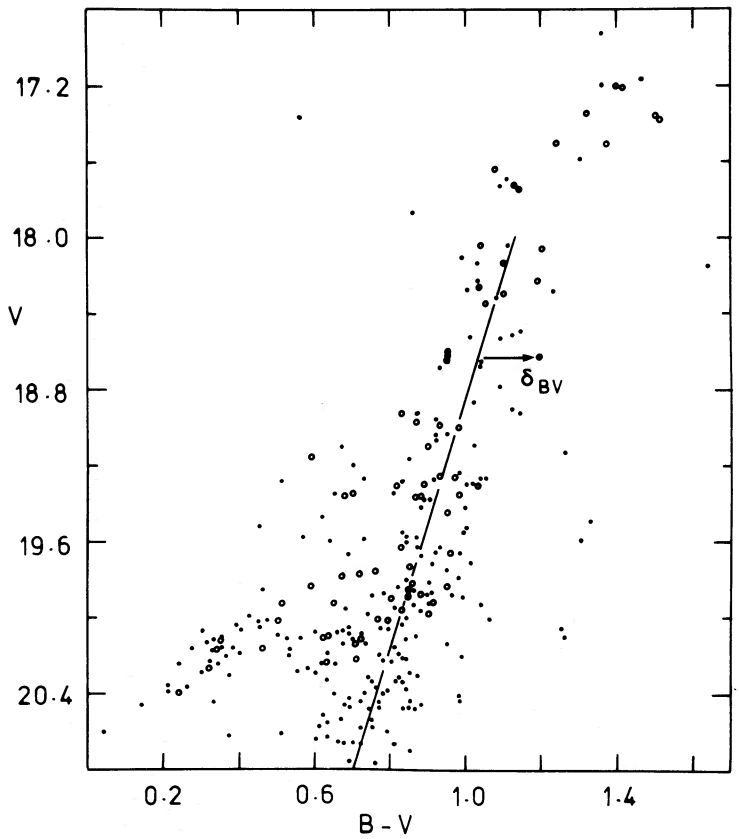

FIG. 5.—The color-magnitude diagram for Sculptor is shown, with every star in Table 4 of Kunkel and Demers (1977) being represented. The stars observed in the present work are depicted by open circles. Also drawn is a fiducial giant branch locus.

important result of the present work. Only four out of 36 (i.e., 11%) Sculptor stars with $V < 19.6$ show greatly enhanced CN, but in contrast, as many as 50% of the giants in clusters such as NGC 6752 (Norris *et al.* 1981) and 47 Tuc (Norris and Freeman 1979) exhibit strengthened CN bands. In clusters such as M5 (Smith and Norris 1983), and notably M13 (Suntzeff 1981), the percentage of CN-rich (first ascent) red giants is much greater.

As a result of the small number of CN-enriched stars in Sculptor, the cyanogen distribution by itself is not distinctive enough to be classified as either ω Cen–like or bimodal. In order to further compare the Sculptor inhomogeneities with those in the globular clusters, the calcium data must be considered. A plot of s_{Ca} versus V for Sculptor is shown in Figure 8. A reference baseline, chosen to be

$$s_{Ca,0} = -0.205V + 3.899 ,$$

is also drawn in. The generalized histogram of δs_{Ca} calcium excess indices, measured relative to this line, is shown in Figure 9, a Gaussian kernel of 0.06 dispersion being employed. The mean δs_{Ca} for the entire sample of stars is 0.276, with a standard deviation of $\sigma_{Ca} = 0.165$. Taking the observed s_{Ca} values to have an uncertainty of 0.12 (standard deviation), the intrinsic standard deviation σ_i is assumed to be given by the relation

$$\sigma_{Ca}{}^2 = \sigma_i{}^2 + 0.12^2 ,$$

which produces $\sigma_i = 0.11$. This suggests that intrinsic s_{Ca} differences, comparable to the observational errors, exist among the Sculptor giants.

A very direct test of whether the present data reflect real calcium abundance variations is to see whether the calcium excess correlates with a $B-V$ color excess,

$$\delta_{BV} = (B-V) - (B-V)_m ,$$

measured relative to the mean giant branch sequence, as shown in Figure 5. The spectra of Norris and Bessell (1978) indicate that the metal abundance in Sculptor ranges from M92–like to M3–like, i.e., from [Fe/H] = −2.3 to −1.7 (Zinn 1980*a*). Over such an abundance range at constant V magnitude, the m_{HK} calcium index of Suntzeff (1980) increases monotonically with [Fe/H], which in turn determines the giant branch color. The plot of δs_{Ca} versus δ_{BV} is shown in Figure 10, which includes only stars with $18.0 < V < 19.5$, because of the large errors incurred in s_{Ca} at fainter magnitudes (see Fig. 4), and because the giant branch is poorly defined for $V < 18.0$. A correlation is apparent, with a correlation coefficient of 0.57, which means that the null

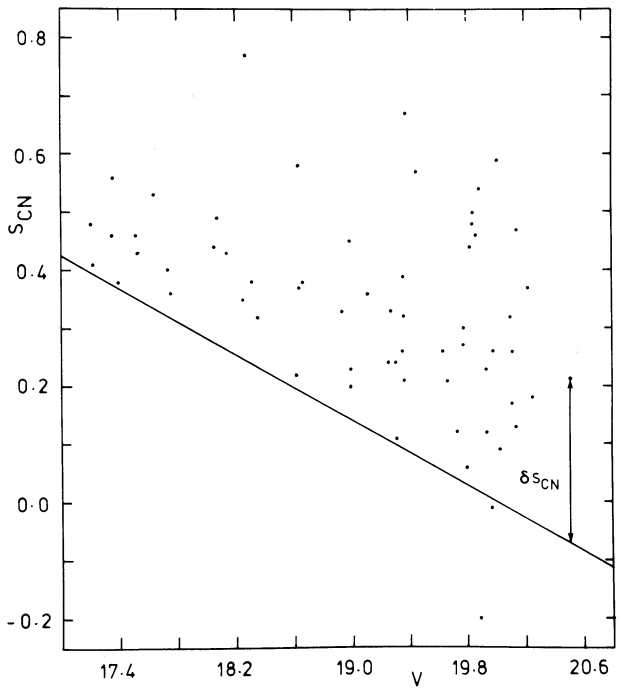

FIG. 6.—A plot of s_{CN} versus V for the non-horizontal branch stars observed. A fiducial baseline is also included, relative to which the cyanogen excess parameter δs_{CN} is measured, as indicated in the diagram.

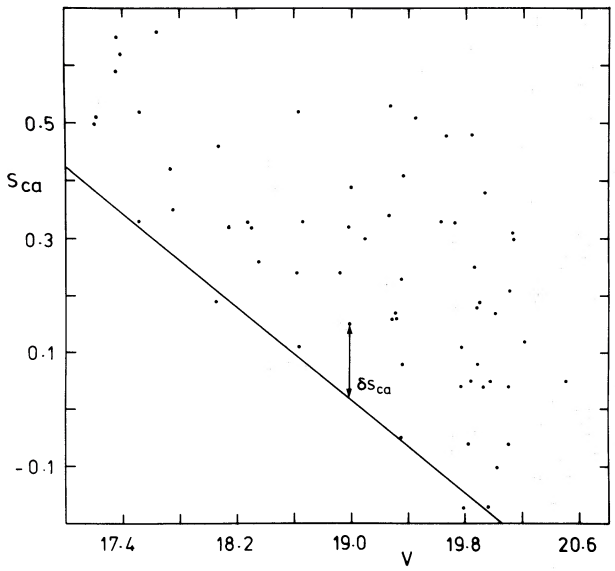

FIG. 8.—The plot of s_{Ca} versus V for the non-horizontal branch stars with s_{Ca} values given in Table 1. The fiducial baseline is drawn in, and the definition of the δs_{Ca} calcium excess parameter illustrated.

hypothesis of no correlation is rejected at the 0.005 level of significance. The second important result of this work is therefore that like the globular clusters ω Cen and M22, and the Draco, Ursa Minor, and Fornax dwarf spheroidal galaxies, Sculptor is chemically inhomogeneous in [Ca/H], and so also presumably in [Fe/H].

At this point it is necessary to make a comment on the possibility of field star contamination in the Sculptor fields. Using data from Allen (1973), and the solar neighborhood spectral type distribution of Jones *et al.* (1981), it is estimated that in the magnitude and color ranges $18 < V < 19.5$, $0.65 < B-V < 1.2$, a total of ~ 2 field stars (assumed to be dwarfs) can be expected in the combined fields 1 and 2. The galactic disk model of Jones *et al.* (1981) predicts that ~ 1 field dwarf would be expected. While it would be valuable to obtain membership data such as radial velocities, or measurements of the λ5211 MgH band strengths as used by Zinn (1978), it is not practical to do so individually for a sample of 70 very faint stars. The above calculations, however, indicate that the conclusions of this work should not be affected by the lack of such information.

The further extent of the similarity of Sculptor to ω Cen and M22 is revealed by Figure 11, which shows a correlation between δs_{CN} and δs_{Ca}, only stars with $V < 19.5$ being represented. The correlation coefficient

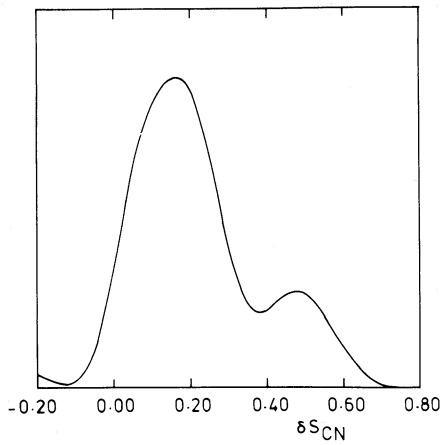

FIG. 7.—The generalized histogram of the cyanogen excess δs_{CN} indices for the non-horizontal branch stars.

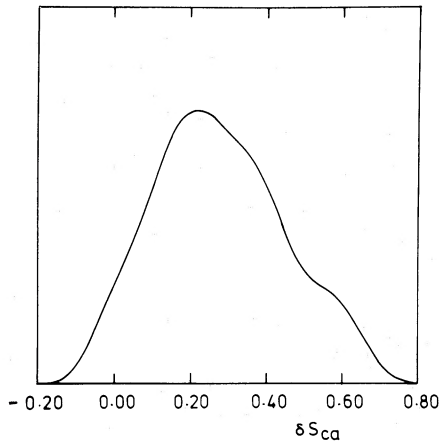

FIG. 9.—The generalized histogram of δs_{Ca} for the non-horizontal branch stars.

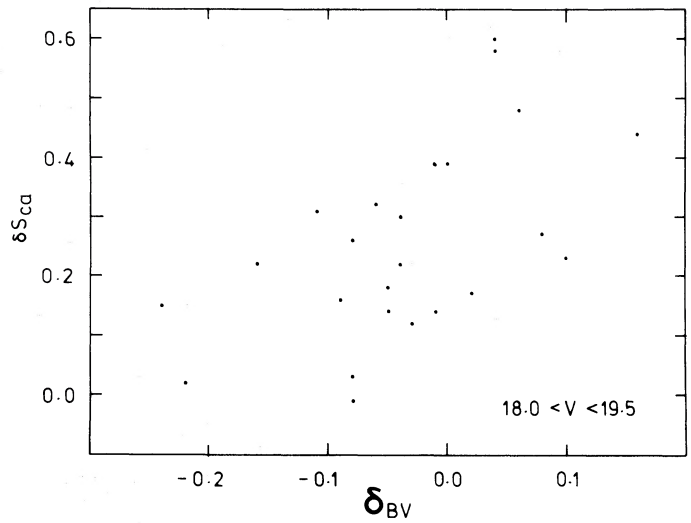

FIG. 10.—This plot illustrates the correlation between δs_{Ca} and δ_{BV}, for stars with $18.0 < V < 19.5$

is 0.46, and the hypothesis that these two parameters are uncorrelated can be rejected at the 0.005 level of significance. A similar connection between cyanogen and calcium variations has been found among the giants in ω Cen (Norris 1980) and M22 (Norris and Freeman 1983). These data provide strong support for the conjecture of Norris and Bessell (1978) that Sculptor exhibits the "ω Cen anomaly." It is possible, however, that star 314, with $\delta s_{CN} = 0.53$ and $\delta s_{Ca} = 0.18$, does not fit into this categorization, since its calcium excess appears to be too small for its cyanogen excess.

The most plausible explanation for the observed inhomogeneities is that they existed at the time of star formation within Sculptor. This indicates two possibilities, as discussed by Zinn (1981).

1. The stars responsible for the earliest heavy-element production in the halo may have been widely separated in the remote regions where the dwarf spheroidals formed. If in addition the outer proto-halo gas was relatively quiescent, the metal-enriched material ejected by these stars may have mixed together only poorly, resulting in a very inhomogeneous halo. These inhomogeneities may have been preserved throughout the fragmentation and collapse of the large clouds from which the dwarf spheroidals formed. In this picture the inhomogeneities were established prior to any star formation in Sculptor.

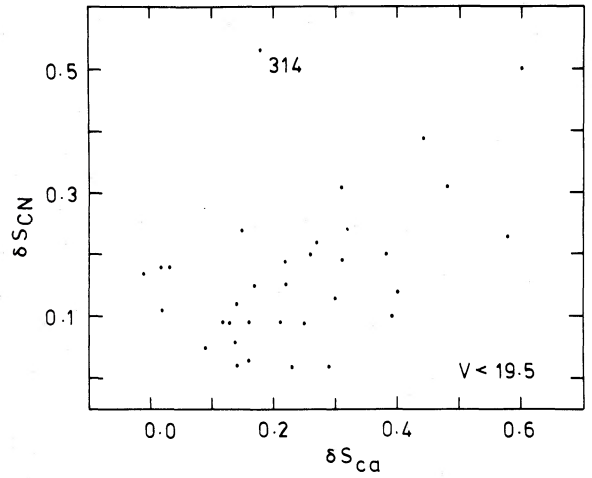

FIG. 11.—This plot illustrates the correlation between δs_{Ca} and δs_{CN}, for stars with $V < 19.5$.

2. Alternatively, a number of massive stars which formed early during the collapse of Sculptor may have expelled enriched material back into their gaseous environment while star formation was still in progress. The supernova explosions which form an integral part of this process eventually produced a cessation of star formation, and a sweeping of gas from Sculptor. Such a picture of galactic self-enrichment has been modeled by Larson (1974), who finds that it is capable of producing metal abundance gradients within galaxies. In addition, Saito (1979) has suggested that virial expansion following sudden gas removal may account for the low central concentrations of the dwarf spheroidals.

Spectroscopic observations are needed to identify the cause of the cyanogen enhancements in some of the Sculptor giants, i.e., are they a consequence of an enhancement in the atmospheric abundance of carbon, or of nitrogen? This question is of interest in view of the discovery of CH stars in Sculptor (Westerlund 1979; Frogel *et al.* 1982). In addition, it would be valuable to obtain low-resolution spectra to investigate whether other strong features such as the Mg *b* and Na D lines vary.

In summary, the following facts have resulted from the present work:

1. The Sculptor dwarf spheroidal galaxy possesses cyanogen-enhanced giants, although not to the same extent as the globular clusters ω Cen, M22, and NGC 6752, for example.

2. The Sculptor giants of similar luminosity display variations in the Ca II H and K line strengths. In this respect, the Sculptor and Draco systems are similar.

3. The cyanogen and calcium anomalies are correlated, as is the case with ω Cen and M22.

The authors are indebted to Dr. E. B. Newell for his advice on running the APEX program and also with regard to the techniques of panoramic photometry. We have also benefited from helpful discussions with Dr. John Norris. We are most grateful to the Director and staff of the Anglo-Australian Observatory for the use of their facilities. Graeme Smith acknowledges the support of a Commonwealth Postgraduate Research Award.

REFERENCES

Allen, C. W. 1973, *Astrophysical Quantities* (3d ed.; London: Athlone Press).
Bessell, M. S., and Norris, J. 1976, *Ap. J.*, **208**, 369.
Boksenberg, A. 1972, Proc. ESO/CERN Conference on Auxiliary Instrumentation for Large Telescopes, Geneva, p. 295.
Butler, D., Dickens, R. J., and Epps, E. 1978, *Ap. J.*, **225**, 148.
Canterna, R., and Schommer, R. A. 1978, *Ap. J. (Letters)*, **219**, L119.
Cohen, J. G. 1981, *Ap. J.*, **247**, 869.
Danziger, I. J. 1973, *Ap. J.*, **181**, 641.
Demers, S., Kunkel, W. E., and Hardy, E. 1979, *Ap. J.*, **232**, 84.
Freeman, K. C., and Norris, J. 1981, *Ann. Rev. Astr. Ap.*, **19**, 319.
Freeman, K. C., and Rodgers, A. W. 1975, *Ap. J. (Letters)*, **201**, L71.
Frogel, J. A., Blanco, V. M., McCarthy, M. F., and Cohen, J. G. 1982, *Ap. J.*, **252**, 133.
Gratton, R. G. 1982, *Astr. Ap.*, **115**, 336.
Harris, H. C., and Canterna, R. 1977, *A.J.*, **82**, 798.
Hartwick, F. D. A., and McClure, R. D. 1974, *Ap. J.*, **193**, 321.
Hesser, J. E., and Harris, G. L. H. 1979, *Ap. J.*, **234**, 513.
Jones, T. J., Ashley, M., Hyland, A. R., and Ruelas-Mayorga, A. 1981, *M.N.R.A.S.*, **197**, 413.
Keeping, E. S. 1962, *Introduction to Statistical Inference* (Princeton: Van Nostrand), p. 202.
Kinman, T. D., Carbon, D. F., Suntzeff, N. B., and Kraft, R. P. 1981, in *IAU Colloquium 68, Astrophysical Parameters for Globular Clusters*, ed. A. G. Davis Philip and D. S. Hayes (Schenectady: L. Davis Press), p. 451.
Kinman, T. D., Kraft, R. P., and Suntzeff, N. B. 1980, in *Physical Processes In Red Giants*, ed. A. Renzini and I. Iben, Jr. (Dordrecht: Reidel), p. 71.
Kraft, R. P. 1979, *Ann. Rev. Astr. Ap.*, **17**, 309.
Kunkel, W. E., and Demers, S. 1977, *Ap. J.*, **214**, 21.
Larson, R. B. 1974, *M.N.R.A.S.*, **169**, 229.
Mallia, E. A., and Pagel, B. E. J. 1981, *M.N.R.A.S.*, **194**, 421.
McClure, R. D. 1979, *Mem. Soc. Astr. Italiana*, **50**, 15.
Newell, E. B. 1979, in *Image Processing in Astronomy*, ed. G. Sedmark, N. Cappacioli and R. J. Allen (Trieste: Osservatorio Astronomico di Trieste), p. 100.
Norris, J. 1980, in *Globular Clusters*, ed. D. Hanes and B. Madore (Cambridge: Cambridge University Press), p. 113.
Norris, J., and Bessell, M. S. 1978, *Ap. J. (Letters)*, **225**, L49.
Norris, J., Cottrell, P. L., Freeman, K. C., and Da Costa, G. S. 1981, *Ap. J.*, **244**, 205.
Norris, J., and Freeman, K. C. 1979, *Ap. J. (Letters)*, **230**, L179.
———. 1983, *Ap. J.*, **266**, 130.
Norris, J., and Smith, G. H. 1981, in *IAU Colloquium 68, Astrophysical Parameters for Globular Clusters*, ed. A. G. Davis Philip and D. S. Hayes (Schenectady: L. Davis Press), p. 109.
Pilachowski, C., Wallerstein, G., Leep, E. M., and Peterson, R. C. 1982, *Ap. J.*, **263**, 187.
Renzini, R. 1977, in *Advanced Stages In Stellar Evolution*, ed. P. Bouvier and A. Maeder (Sauverny: Geneva Observatory), p. 149.
Rodgers, A. W., Freeman, K. C., Harding, P., and Smith, G. H. 1979, *Ap. J.*, **232**, 169.
Saito, M. 1979, *Pub. Astr. Soc. Japan*, **31**, 193.
Schommer, R. A., Olszewski, E. W., and Cudworth, K. M. 1981, in *IAU Colloquium 68, Astrophysical Parameters for Globular Clusters*, ed. A. G. Davis Philip and D. S. Hayes (Schenectady: L. Davis Press), p. 453.
Schommer, R. A., Olszewski, E. W., and Kunkel, W. E. 1977, in *IAU Symposium 80, The HR Diagram*, ed. A. G. Davis Philip and D. S. Hayes (Dordrecht: Reidel), p. 269.
Searle, L., and Zinn, R. 1978, *Ap. J.*, **225**, 357.
Smith, G. H. 1983, *A.J.*, **88**, 410.
Smith, G. H., and Norris, J. 1982, *Ap. J.*, **254**, 149.
———. 1983, *Ap. J.*, **264**, 215.
Stetson, P. B. 1979, *A.J.*, **84**, 1149.
———. 1980, *A.J.*, **85**, 398.
Suntzeff, N. B. 1980, *A.J.*, **85**, 408.
———. 1981, *Ap. J. Suppl.*, **47**, 1.
van den Bergh, S. 1969, *Ap. J. Suppl.*, **19**, 145.
Westerlund, B. E. 1979, *ESO Messenger*, **19**, 7.
Zinn, R. 1978, *Ap. J.*, **225**, 790.
———. 1980*a*, *Ap. J.*, **241**, 602.
———. 1980*b*, *A.J.*, **85**, 1468.
———. 1981, *Ap. J.*, **251**, 52.
Zinn, R., and Persson, S. E. 1981, *Ap. J.*, **247**, 849.

MICHAEL A. DOPITA: Mount Stromlo & Siding Spring Observatories, Private Bag, WODEN. P.O. ACT 2606, Australia

GRAEME H. SMITH: Harvard-Smithsonian Center for Astrophysics, 60 Garden Street, Cambridge, MA 02138